Check for updates

# Sensitive distance-based paper-based quantification of mercury ions using carbon nanodots and heating-based preconcentration†

Benjawan Ninwong,[ab] Prapaporn Sangkaew,[a] Photcharapan Hapa,[a] Nalin Ratnarathorn,[a] Ruth F. Menger,[c] Charles S. Henry [iD][c] and Wijitar Dungchai [iD] *[ad]

This article reports the first fluorescent distance-based paper device coupled with an evaporating preconcentration system for determining trace mercury ions (Hg$^{2+}$) in water. The fluorescent nitrogen-doped carbon dots (NCDs) were synthesized by a one-step microwave method using citric acid and ethylenediamine. The fluorescence turn-off of the NCDs in the presence of Hg$^{2+}$ was visualized with a common black light, and the distance of the quenched fluorescence correlated to Hg$^{2+}$ concentration. The optimal conditions for pH, NCD concentration, sample volume, and reaction time were investigated. Heating preconcentration was used to improve the detection limits of the fluorescent distance-based paper device by a factor of 100. Under the optimal conditions, the naked eye limit of detection (LOD) was 5 μg L$^{-1}$ Hg$^{2+}$. This LOD is sufficient for monitoring drinking water where the maximum allowable mercury level is 6 μg L$^{-1}$ as established by the World Health Organization (WHO). The fluorescent distance-based paper device was successfully applied for Hg$^{2+}$ quantification in water samples without interference from other cations. The proposed method provides several advantages over atomic absorption spectroscopy including ease of use, inexpensive material and fabrication, and portability. In addition, the devices are simple to fabricate and have a long shelf-life (>5 months).

## 1. Introduction

Heavy metals are important components of many manufacturing processes. In industrial manufacturing, heavy metals are used as raw materials for the conductive parts of batteries and for catalysts during plastic production. In the agricultural sector, heavy metals are used in the manufacture of insecticides.[1,2] Heavy metals can leach into surface water and groundwater during manufacturing and product use. The contamination of heavy metals in the environment is a serious problem as they are harmful to humans and the environment.[3,4] Mercury is one of the toxic metals which can exist in elemental,

organic, and inorganic forms. The inorganic form of Hg$^{2+}$ is the most common form found in drinking water and environmental waters.[5,6] Mercury has harmful effects on the nervous, digestive and immune systems, as well as the lungs, kidneys, skin, and eyes. The maximum allowable Hg$^{2+}$ level in drinking water is 6 μg L$^{-1}$ as established by the World Health Organization (WHO). Therefore, a highly sensitive method for mercury detection is necessary to protect and control the distribution of mercury in food and the environment.[7,8]

Standard methods for Hg$^{2+}$ detection include atomic absorption spectroscopy (AAS), inductively coupled plasma-atomic emission spectroscopy (ICP-AES), inductively coupled plasma-mass spectrometry (ICP-MS), and fluorescence spectroscopy.[9–12] AAS, ICP-AES, and ICP-MS are commonly used because of their high sensitivity but are large, extremely costly, and laboratory-based instruments. Fluorescence-based sensing has received much attention due to its high selectivity, high sensitivity, speed, and cost-effectiveness. Several fluorescent materials have been developed using organic dyes, quantum dots, metal–organic frameworks, and fluorescent proteins.[13,14] Zhang *et al.*[15] developed a simple, low-cost, one-pot hydrothermal method to synthesize nitrogen-doped carbon nanodots (NCDs) for turn on-off fluorescence sensing of Hg$^{2+}$ and L-cysteine. Hg$^{2+}$ can completely quench the fluorescence of NCDs by the formation of a stable, non-fluorescent NCD–Hg$^{2+}$ complex.

*[a]Organic Synthesis, Electrochemistry & Natural Product Research Unit, Department of Chemistry, Faculty of Science, King Mongkut's University of Technology Thonburi, Prachautid Road, Thungkru, Bangkok, 10140, Thailand. E-mail: wijitar.dun@kmutt.ac.th; Fax: +66-2-470-8840; Tel: +66-2-470-9553*

*[b]Nanomaterials Chemistry Research Unit, Department of Chemistry, Faculty of Science and Technology, Nakhon Si Thammarat Rajabhat University, Nakhon Si Thammarat, 80280, Thailand*

*[c]Departments of Chemistry and Chemical & Biological Engineering, Colorado State University, Fort Collins, CO 80523, USA*

*[d]Applied Science & Engineering for Social Solution Unit, Faculty of Science, King Mongkut's University of Technology Thonburi, Prachautid Road, Thungkru, Bangkok, 10140, Thailand*

† Electronic supplementary information (ESI) available. See DOI: 10.1039/d0ra00791a

He et al.[16] also developed a fluorescent probe using NCDs for determination of $Hg^{2+}$ and $I^-$ in real lake water and urine samples demonstrating a simple, sensitive, and robust method. NCDs are an interesting material for fluorescent sensing due to advantages such as water solubility, chemical inertness, low toxicity, ease of functionalization, and resistance to photobleaching.[17-21] However, the detection with NCDs still requires a fluorimeter and a highly skilled scientist.

Recently, paper-based analytical devices (PADs) or microfluidic paper-based analytical devices (μPADs) have been developed as an instrument-free analysis technique.[22,23] μPADs are an alternative to traditional laboratory instrumentation for point-of-care monitoring due to minimal sample requirements, environmental friendliness, and rapid analysis. Moreover, the techniques used to fabricate μPADs are inexpensive. Although many μPAD applications have emerged over the last decade in fields such as diagnostics, biological samples, food safety, and environmental analysis,[24-30] μPADs continue to be developed for various aspects of metal detection. Kim et al.[31] reported a new fluorescent method for $Al^{3+}$ and $Hg^{2+}$ detection using a paper-based sensor strip containing tethered rhodamine carbon nanodots. The sensor could efficiently detect $Al^{3+}$ over other metal ions via forester resonance energy transfer (FRET). Sensing based on FRET of NCDs is color-tunable and can be identified with the naked eye, providing a new platform for specific metal-ion sensing. Unfortunately, the method still suffers from low sensitivity with limits of detection for $Al^{3+}$ [31] and $Hg^{2+}$ [32] at around 1 mg $L^{-1}$. These levels are insufficient for monitoring aluminum and mercury in drinking water where the maximum allowable aluminum and mercury levels established by the WHO are at 0.1 and 6 μg $L^{-1}$, respectively.[33]

To obtain a lower limit of detection, preconcentration steps can be applied to μPADs. Several methods have been reported for preconcentration and monitoring of trace heavy metals by solid-phase extraction[34] and of biological molecules by evaparation.[35] Wong et al. used the evaporation process to concentrate a tuberculosis biomarker on a paper-based device.[35] This method used the application of localized heat to a paper strip causing evaporation of a large sample volume to concentrate the analyte. A paper strip was hung and sandwiched between two aluminum plates which were heated and the bottom of the paper strip was dipped in the sample reservoir. The evaporation process could be suitable for preconcentration of heavy metals but flow through the paper will be slow due to gravity.

Here, we report the first fluorescent distance-based paper device coupled with an evaporation system for determining trace mercury ($Hg^{2+}$) in water. We developed an evaporation system that retains paper shape during preconcentration and avoids reduction in flow rate caused by gravity. The new method improves on previous μPADs[22,32] by allowing for instrument-free signal quantitation and lowering the detection limit of $Hg^{2+}$. Moreover, the proposed method is highly selective, portable, and was successfully applied for mercury detection in drinking, pond, and tap water samples.

## 2. Experimental

### 2.1. Reagents and materials

All chemicals and reagents were obtained from Thermo Scientific, were of analytical grade, and were dissolved in ultrapure water (resistivity ≥ 18.2 MΩ $cm^{-1}$). Citric acid and ethylenediamine were used for NCD synthesis. Four different types of Whatman filter paper were investigated: filter paper no. 1 (cat no. 1001-917), anion exchange filter paper (cat no. 3658-915), cation exchange filter paper (cat no. 3698-915) and silica gel filter paper (cat no. 3668-915). Mercury nitrate ($Hg(NO_3)_2 \cdot H_2O$) was used as a standard solution. Buffer solutions were used to study the pH effect including sodium citrate buffer (pH 3–pH 5), phosphate buffer (pH 6–pH 9), tris-hydrochloric buffer (pH 9) and $Na_2HPO_4$–NaOH buffer (pH 10–pH 12). $FeCl_3 \cdot 6H_2O$, $FeSO_4 \cdot 7H_2O$, $CoCl_2 \cdot 6H_2O$, $NiSO_4 \cdot H_2O$, $MnSO_4 \cdot H_2O$, $Zn(NO_3)_2 \cdot 6H_2O$, $CrCl_3 \cdot 6H_2O$ $Pb(NO_3)_2 \cdot 6H_2O$, $Cd(NO_3)_2 \cdot 3H_2O$, $Al(NO_3)_3 \cdot 9H_2O$, $Cu(NO_3)_2 \cdot 3H_2O$, $AsCl_3$, $BaCl_2$, $CaCl_2$, NaCl and KCl, were used for interference studies. To prevent metal contamination, laboratory glassware was kept overnight in a 10% (v/v) nitric acid solution and rinsed with DI water before use.

### 2.2. Instrumentation

X-ray diffraction (XRD, btx II Olympus), UV-vis spectrophotometry (UV-vis, Lambda 35/FIAS300 PerkinElmer), fluorescence spectroscopy (F-2500 Hitachi), transmission electron microscopy (TEM, Tecni 20 Philip), nanoparticle analyzer (HORIBA Scientific, SZ-100) and Fourier transform infrared spectroscopy (FTIR, NICOLET 6700 Thermo scientific) were used for characterization of the NCDs. A household microwave oven (ME711K, Samsung) was used for NCD synthesis. For the detection of $Hg^{2+}$, a black light from a local market was used in a black acrylic box for illumination (20 cm × 20 cm × 20 cm, Fig. S1†). The results were analyzed by both naked eye and an image collected with a digital camera or smartphone. Method validation was performed by hydride generation atomic absorption spectroscopy (HG-AAS, Analytic Jena). The heater for preconcentration was fabricated in house (Fig. S9†) and consisted of a heating zone (diameter 2.0 cm) and an insulator zone.

### 2.3. Synthesis of NCDs

The NCDs were synthesized according to a simple one-step microwave method.[36] In brief, 2.0 g of citric acid was added to 5 mL ultrapure water followed by 390 μL ethylenediamine to dope nitrogen on the NCD's surface. The mixture solution was then put in the microwave at 680 W for 5 min. After 5 min, a red-brown foamy solid appeared and was purified using a centrifugal filter unit (Nanosep with 3 kDa.). XRD, UV-vis spectroscopy, fluorescence spectroscopy, TEM (Phillip, Tecni20) and FTIR were used to characterize the NCD solution. The NCD solutions were kept at 4 °C prior to use.

### 2.4. Preparation of distance-based paper device

Paper-based devices were made from several types of filter paper: normal Whatman filter paper no. 1, anion exchange filter

paper, cation exchange filter paper, and silica gel filter paper (Whatman). The pattern was designed with CorelDraw X7 and printed onto the paper using a wax printer (Xerox ColorQube 8870, Japan).[37] The printed wax was melted in a convection oven at 115 °C for 5 min. When cooled to room temperature, the absorbed wax formed a hydrophobic barrier defining a channel in the paper. The device has two zones, the (i) sample zone (diameter 5.0 mm) and (ii) detection zone (width 3.5 mm, channel length of 70 mm).

### 2.5. $Hg^{2+}$ detection

Fluorescent distance-based paper devices were prepared for $Hg^{2+}$ detection. The NCDs (10 μL) were dropped onto the detection zone using a pipette and allowed to dry. The $Bi^{3+}$ solution was added to the standard or sample solution to increase the sensitivity of the detection method. For analysis, 75 μL of a standard or sample containing with $Bi^{3+}$ (1 to 20 mg $L^{-1}$) was added to the sample zone. Upon addition of the sample, the fluorescence of the NCDs is turned off due to the formation of a $Hg^{2+}$–NCD complex. The distance of turned off fluorescence positively correlates to the $Hg^{2+}$ concentration. The distance was measured by a luminous ruler (Fig. S1†) under a black light in a black box as shown in Scheme 1. The optimum conditions for paper type, pH solution, NCD concentration, sample volume, and analysis time were studied. Interference from other cations was investigated by comparing the distance signal obtained from just $Hg^{2+}$ to $Hg^{2+}$ mixed with sixteen cation ions: $Cd^{2+}$, $Cr^{3+}$, $As^{3+}$, $Cu^{2+}$, $Pb^{2+}$, $Mn^{2+}$, $Al^{3+}$, $Fe^{3+}$, $Fe^{2+}$, $Co^{2+}$, $Ni^{2+}$, $Zn^{2+}$, $Ba^{2+}$, $K^+$, $Ca^{2+}$ and $Na^+$.

### 2.6. Determination of $Hg^{2+}$ in water samples

To evaluate the utility of the fluorescent distance-based paper device for $Hg^{2+}$ determination with real samples, the amount of $Hg^{2+}$ was quantified in drinking, pond, and tap water. Drinking and tap water were analyzed without pretreatment while pond water was filtered to remove large particles prior to analysis. The accuracy of the method was determined by spiking samples with a standard solution of $Hg^{2+}$ at 2, 12, and 22 mg $L^{-1}$ with additional validation by HG-AAS. The standard preparation method for mercury detection (APHA Method 9221: standard methods for the examination of water and wastewater) was used for HG-AAS.[38] Mercury was reduced to elemental mercury vapor using $NaBH_4$ and HCl as the reducing agents for hydride formation. In order to improve the application of on-site environmental detection, the stability of NCDs was studied. NCDs were added to the device stored at 4 °C in a dark and were used to detect $Hg^{2+}$ after 5 months to evaluate NCD stability.

### 2.7 Heating preconcentration on paper-based microfluidics

The heater for preconcentration was designed in house (Fig. S9†) and consists of a heating zone (diameter 2.0 cm) and an insulating zone. The heater is made of low voltage cartridge heaters (12 volt batteries, 40 watts). The temperature for preconcentration was studied in the range of 50–250 °C. The optimal temperature was 100 ± 1 °C, which resulted in the highest turned-off fluorescence distance.

## 3. Results and discussion

### 3.1. Characterization of NCDs

The optical properties of NCDs were characterized by UV-vis and fluorescence spectroscopy in solution.[39] The UV-vis absorption spectra of NCDs with and without $Hg^{2+}$ at 5 and 10 ppm are shown in Fig. 1a. The spectra indicate the presence of C=O/C–OH or C=N functional groups and n–π* transitions. NCDs dispersed in water appear yellow under ambient light and emit blue fluorescence under a UV lamp (inset of Fig. 1b). Strong fluorescence emission was observed at 450 nm with excitation at 350 nm (Fig. 1b and c). The XRD pattern (Fig. S2†) shows the
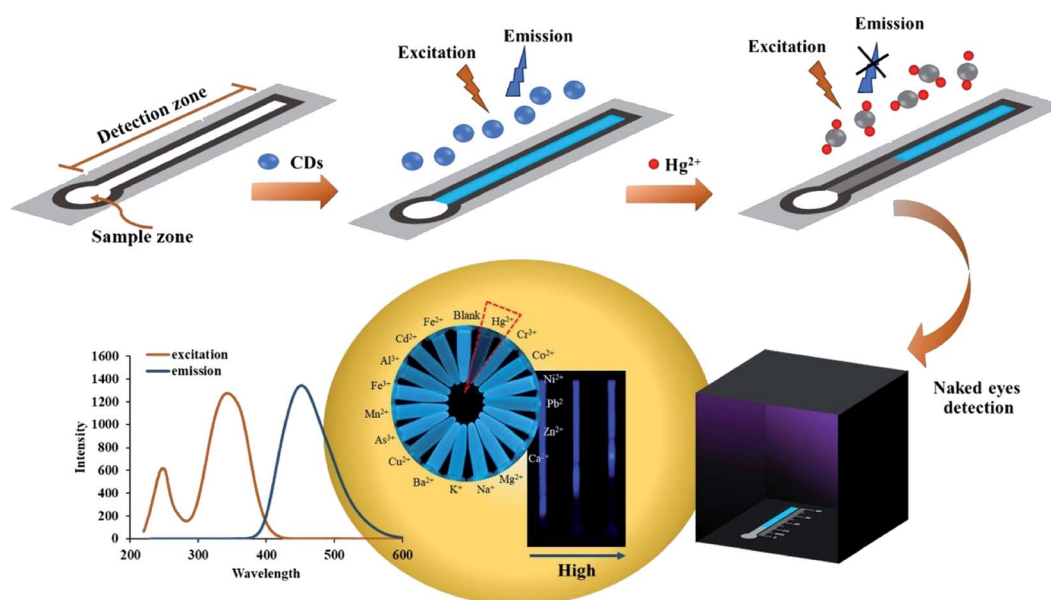


**Scheme 1** Determination of $Hg^{2+}$ by fluorescent distance-based paper device.
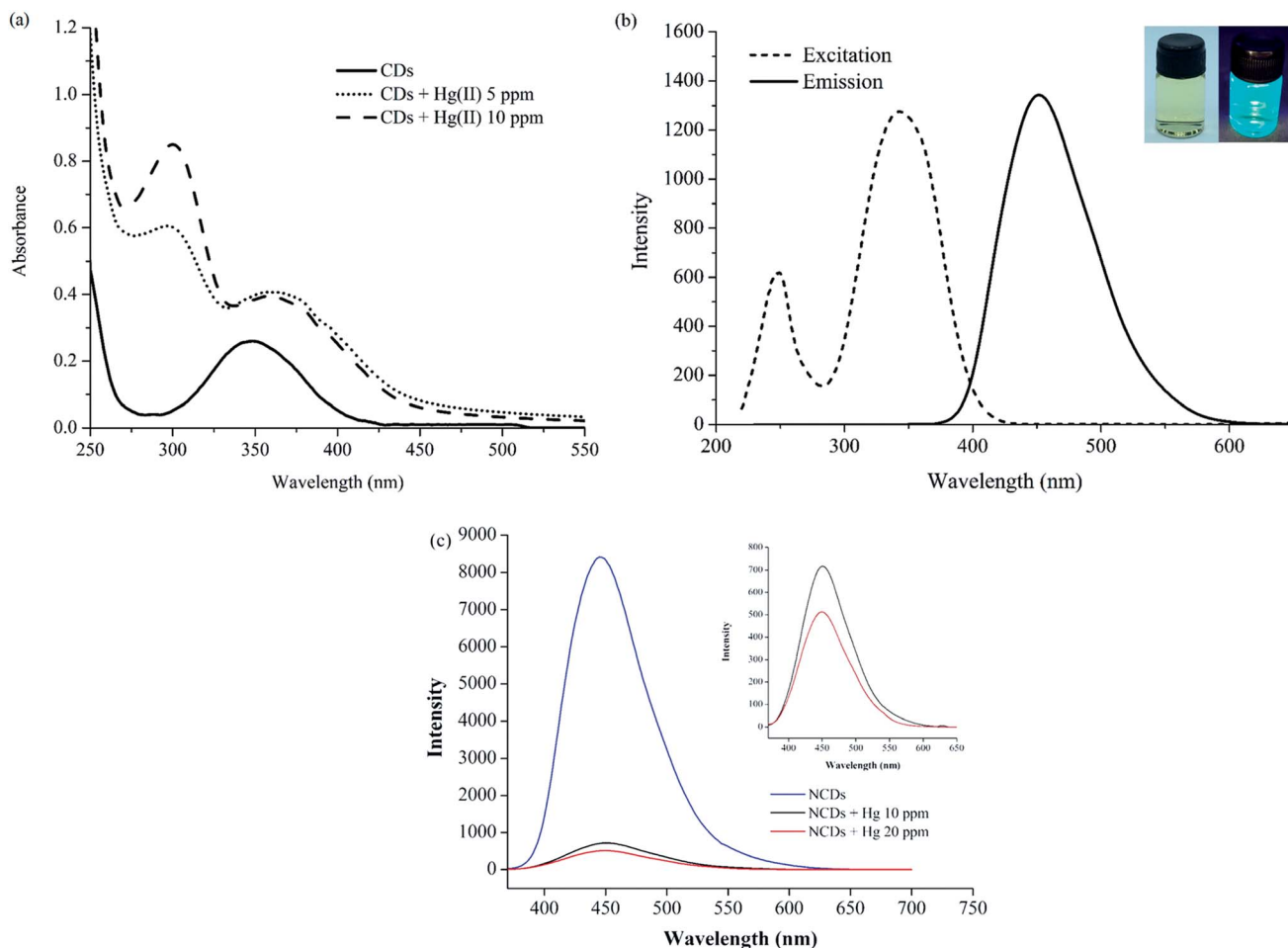
Fig. 1 Characterization of NCDs using UV-visible spectroscopy (a) and fluorescence spectroscopy at 350 nm excitation wavelength (b). Inset: photo of NCDs dispersed in water under ambient light (left) and under a UV lamp (right). Fluorescence emission spectroscopy of NCDs with and without $Hg^{2+}$ at 350 nm excitation wavelength (c).

(002) reflection plane that exhibits a broad diffraction peak at $2\theta = 20°$.[15,40] A study of the functional groups on NCDs was done by FTIR, and the spectra are shown in Fig. S3.† OH-bond stretching at 3490 cm$^{-1}$ and asymmetric stretching of C=O at 1720 cm$^{-1}$ were observed. A peak was also found at 1600 cm$^{-1}$ corresponding to C=O bending and C–C stretching, respectively. Peaks appearing at the 1400 and 1320–1100 cm$^{-1}$ wavenumbers indicated the bending vibration of C–N and C=N from NCDs which were different from the citric acid spectra (Fig. S3†).[41,42] The negative zeta potential of −5.6 mV is also found for the NCDs. TEM images show the good dispersion of NCDs with a narrow size distribution in the range of 2 to 5 nm (Fig. S4a†). The average diameter of the NCDs is 3 nm (Fig. S4b†) whereas the $Hg^{2+}$–NCD complex is about 70 nm (Fig. S4c and d†).[43,44]

## 3.2. $Hg^{2+}$ detection using fluorescent distance-based paper device

The fluorescence turn-off mechanism of NCDs with $Hg^{2+}$ was studied next. The fluorescence on the distance-based paper device is similar to the behavior of NCDs and $Hg^{2+}$ in solution.[15,16,40,45,46] In the UV-vis absorption spectra in Fig. 1a, a new absorption peak appears at 300 nm in the presence of $Hg^{2+}$ and higher absorbance intensity was found with increasing $Hg^{2+}$ concentration. This suggests that $Hg^{2+}$ can bind with the C=O/ C–OH or C=N of the NCDs via covalent bonding between an empty orbital of $Hg^{2+}$ and electrons of NCDs, leading to the formation of a non-fluorescent metal adduct. TEM results confirmed that the particle size of the $Hg^{2+}$–NCD complex was larger than NCDs (Fig. S4c and d†). Ethylenediamine was applied for the modification of CDs in this work because $Hg^{2+}$ has a stronger affinity toward nitrogen on NCDs than other ions.[47] Based on their stronger affinity towards complexation with nitrogen and their large radius, $Hg^{2+}$ ions can affect the fluorescence quenching of NCDs.[47] Different functional groups affect the energy levels of the NCDs, which alter and enhance the light absorption and emissive spectrum of the sensors. For example, Patir et al. modified NCDs with ethylenediaminetetraacetic (EDTA) acid which has a carboxylic acid group so the fluorescence of the EDTA–NCDs was quenched by both $Hg^{2+}$ and $Cu^{2+}$.[48] Unfortunately, the detection limit of the EDTA–NCDs on a paper-based device (20 μg L$^{-1}$) is insufficient for monitoring $Hg^{2+}$ in drinking water, where 6 μg L$^{-1}$ is recommended by the WHO.

(a)



pH 3    pH 4    pH 5    pH 6    pH 7    pH 8    pH 9    pH 10   pH 11   pH 12

(b)



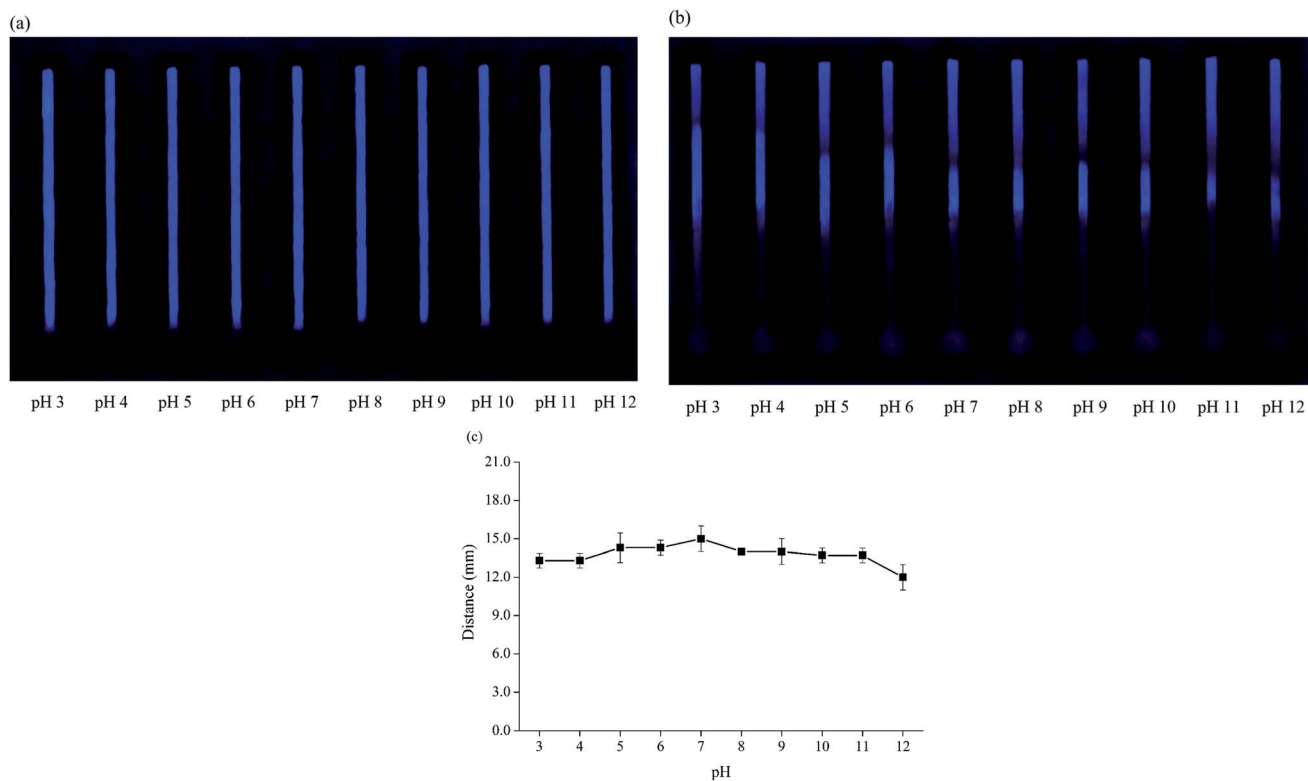pH 3    pH 4    pH 5    pH 6    pH 7    pH 8    pH 9    pH 10   pH 11   pH 12

(c)



**Fig. 2** pH effect on fluorescent distance-based paper device with blank (a) and in the presence of 10 mg $L^{-1}$ $Hg^{2+}$ (b and c).

Thus, the fluorescence quenching caused by the interaction between $Hg^{2+}$ and our NCDs was applied to the distance-based paper device for simpler and easier detection.

### 3.3. Optimized conditions

**3.3.1 Paper types.** The effect of paper type on the fluorescent signal was studied next. Whatman no. 1 filter paper, anion exchange filter paper, cation exchange filter paper and silica gel filter paper were all tested to determine the optimal paper surface. The results indicate that only anion exchange filter paper can be used for the fluorescent distance-based detection. With other paper types, the fluorescence signal was not different between the blank and $Hg^{2+}$. The NCDs could be immobilized on the anion exchange paper because the positive charges of diethylaminoethyl cellulose on the paper surface interact with the negative charge of the functional groups on the NCDs. NCDs on other paper types were not immobilized after addition of the blank and 10 mg $L^{-1}$ $Hg^{2+}$ solution, instead flowing through the channel so the length of fluorescence quenching between the presence and absence of $Hg^{2+}$ could not be distinguished by naked eye. Based on these results (Fig. S5†), anion exchange filter paper was selected for the determination of $Hg^{2+}$ in the remaining experiments.

**3.3.2 Effect of pH.** The influence of pH was evaluated from pH 3 to 12 standard buffer solutions (Fig. 2). The length of quenched fluorescence on the paper device in the presence of 10 mg $L^{-1}$ $Hg^{2+}$ was not significantly different from pH 3 to pH 11 (Fig. 2b, ANOVA, $p > 0.05$). At pH 12, the distance signal

significantly decreased because $Hg^{2+}$ could form a hydroxide complex with the $OH^-$ in basic solution. Moreover, the $pK_a$ of diethylaminoethyl on paper is 11.50 so anion exchange filter paper should be used at a pH below the $pK_a$ of the amine group to maintain a positive charge on the paper. We also found that the fluorescence of NCDs in solution is highly sensitive towards pH due to the formation of aggregates at low pH. After NCDs were immobilized on the anion exchange filter paper however, the aggregation of NCDs did not occur as we did not find a decrease in fluorescence at low pH. From this result, one advantage of our proposed technique is the robustness of $Hg^{2+}$ detection to various pH conditions compared to previous works.[18,48] In this work, DI water was used for sample preparation to maintain a suitable pH that would match the real samples.[15]

**3.3.3 Influence of NCD concentration.** The concentration of NCDs was investigated in the range of 3–11 g $L^{-1}$ (Fig. S6†). An NCD concentration of 5 g $L^{-1}$ was chosen because it provided the most significant difference between fluorescence and turn-off fluorescence signal by naked-eye detection. Although 9 g $L^{-1}$ had the highest turn-off length, the contrast between the regular and quenched zones was not as great as in the 5 g $L^{-1}$ devices, likely due to quenching of NCDs at these higher levels. At lower concentrations of NCDs, the observation between fluorescence signal of blank and turned off signal from analyte was difficult to distinguish by naked eye. Therefore, an NCD concentration of 5 g $L^{-1}$ was used for this device.
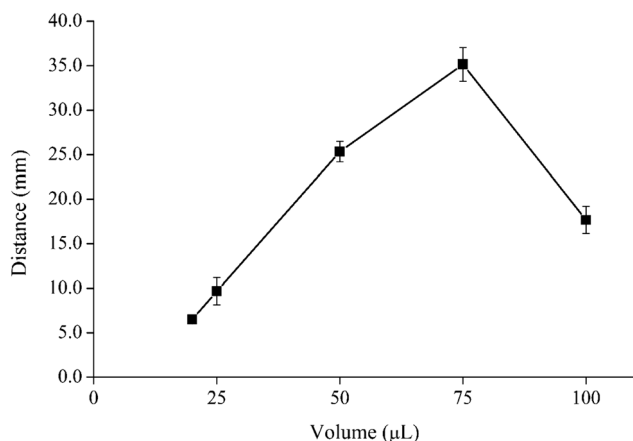
**Fig. 3** Effect of volume in the range of 20–100 μL with 10 mg L$^{-1}$ of Hg$^{2+}$.

**3.3.4 Sample volume and analysis time.** The effect of sample volume was investigated in the range of 20 to 100 μL using 10 mg L$^{-1}$ of Hg$^{2+}$. A sample volume at 75 μL was found to give the highest distance signal (Fig. 3). For the lower volumes, the sample did not fully wet the device. At 100 μL, the signal decreased because the sample solution leaked out of the sample zone and didn't flow through the channel. Therefore, the maximum sample volume is 75 μL. The suitable time for mercury detection at this maximum volume was 40 min (Fig. 4). The fluorescent signal on the distance-based device did not change significantly after 40 min (ANOVA, $p > 0.05$).

**3.3.5 Effect of Bi$^{3+}$ concentration.** NCDs are negatively charged due to the abundant C=O/C–OH or C=N functional groups on their surface so the electrostatic interactions between the functional groups on the NCD surface and Bi$^{3+}$ could offer a driving force for the assembly of a bimetallic Hg$^{2+}$ and Bi$^{3+}$ complex with the NCDs.[49,50] We found that Bi$^{3+}$ by itself did not turn off the fluorescence signal ($I_0/I = 1$, $I_0$ and $I$ are the NCDs before and after adding the metal solution) whereas the bimetallic Hg$^{2+}$ and Bi$^{3+}$ can enhance the ratio of $I_0/I$ compared to only Hg$^{2+}$ from 11.7 (only Hg$^{2+}$) to 12.6 (Hg$^{2+}$ and Bi$^{3+}$)
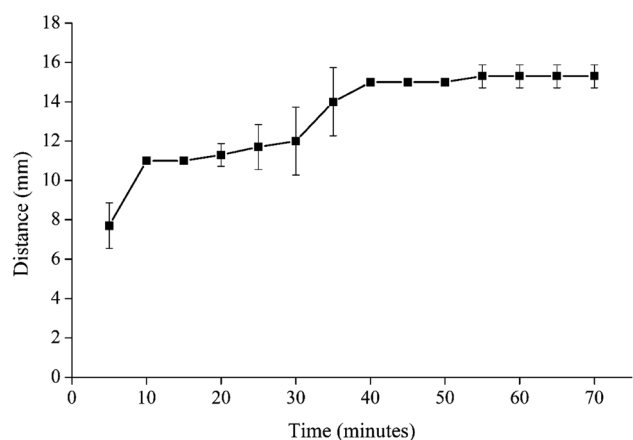
(Fig. S7a†). To increase the sensitivity of the detection method, Bi$^{3+}$ was added to the standard or sample solution. Thus, the effect of Bi$^{3+}$ concentration was studied in the range of 1 to 20 mg L$^{-1}$ with 10 mg L$^{-1}$ of Hg$^{2+}$. As the Bi$^{3+}$ concentration increased up to 10 mg L$^{-1}$, the quenched fluorescence distance signal increased, and after 10 mg L$^{-1}$ the distance signal plateaued (Fig. S7(b)†). Therefore, the suitable Bi$^{3+}$ concentration was chosen at 10 mg L$^{-1}$.

### 3.4. Interference study

The effect of interfering ions on the fluorescent distance-based paper device was investigated in ratios of 1 : 1, 1 : 5 and 1 : 100 analyte to interference with the concentration of Hg$^{2+}$ at 10 mg L$^{-1}$. The analytical response recovery of the solution containing only Hg$^{2+}$ was compared with the addition of the cation interferences. It was found that none of the cations including Cd$^{2+}$, Cr$^{3+}$, As$^{3+}$, Cu$^{2+}$, Pb$^{2+}$, Mn$^{2+}$, Al$^{3+}$, Fe$^{3+}$, Fe$^{2+}$, Co$^{2+}$, Ni$^{2+}$, Zn$^{2+}$, Ba$^{2+}$, K$^+$, Ca$^{2+}$, and Na$^+$ affected the performance of the fluorescent distance-based paper device at ratios of 1 : 1 and 1 : 5 as defined by a change of <10% (Fig. 5). At a ratio of 1 : 100 of Cu$^{2+}$, Pb$^{2+}$, Al$^{3+}$, Fe$^{3+}$, and Fe$^{2+}$ did influence the off-fluorescence signal (Fig. S8†). The result showed that our proposed device has high selectivity for Hg$^{2+}$ except for with Cu$^{2+}$, Pb$^{2+}$, Al$^{3+}$, Fe$^{3+}$ and Fe$^{2+}$ at the 1 : 100 ratio because Hg$^{2+}$ has a larger ionic radius and polarization when compared to other metal ions as well as a greater ability to form complexes
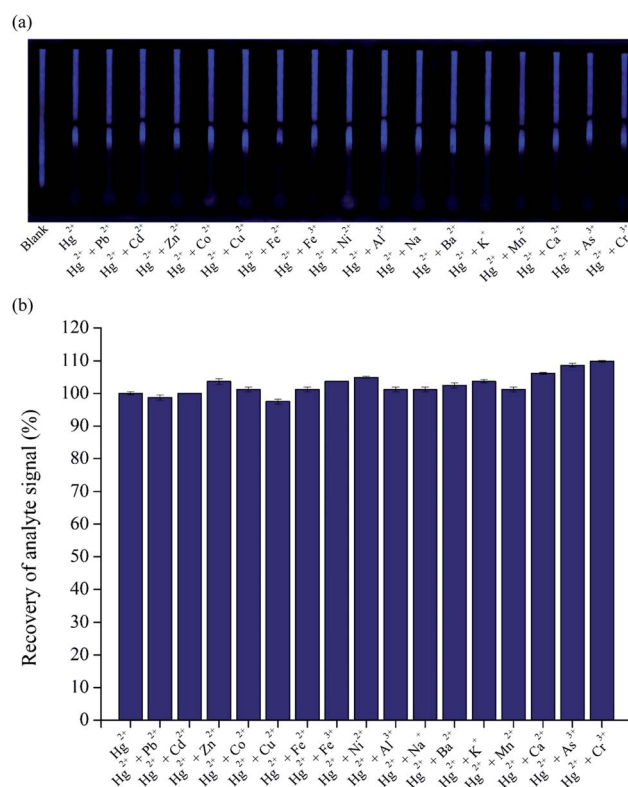


**Fig. 5** Interferences effect with 1 : 1 ratio of analyte to interference in 10 mg L$^{-1}$ at difference metals ion under black light image (a) and the analytical response recovery graph (b).
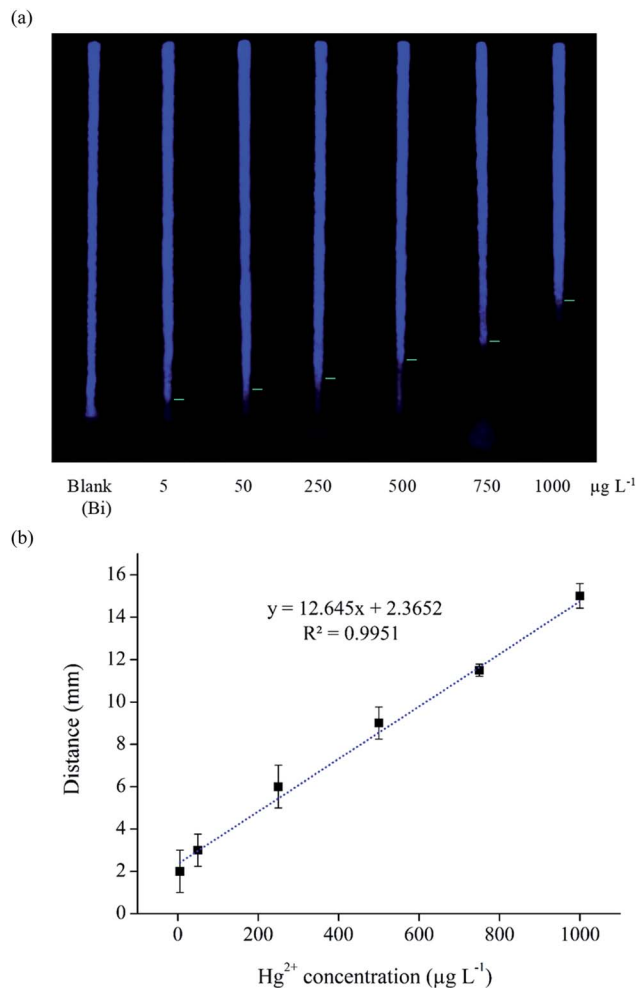


**Fig. 4** Effect of time in the range of 5–70 min with 10 mg L$^{-1}$ of Hg$^{2+}$.

(a)



Blank 5 50 250 500 750 1000 μg L$^{-1}$
(Bi)

(b)



$y = 12.645x + 2.3652$
$R^2 = 0.9951$

**Fig. 6** Heating preconcentration for determination of Hg$^{2+}$ using fluorescent distance-based paper device with the image under black light (a) and calibration curve in the range 0.005–1 mg L$^{-1}$ (b).

with nitrogen.[47] Therefore, the deformation of Hg$^{2+}$ happens more easily when it interacts with the negative functional group of NCDs.[39,47]

### 3.5. Analytical performance

Under the optimum conditions without heating preconcentration, the linear range was 0.5 to 25 mg L$^{-1}$ ($R^2 = 0.9952$, Fig. S10†). The relative standard deviations (%RSD) at 5 and 25 mg L$^{-1}$ were 8.5% and 6.7%, respectively ($n = 10$), which is acceptable for paper-based devices. The naked eye detection limit (LOD) was found to be 0.5 mg L$^{-1}$. The LOD of this developed method is comparable to the paper-based colorimetric quantification developed by Cai *et al.*[32] which was 0.93 mg L$^{-1}$ for Hg$^{2+}$ detection. In the method developed by Cai *et al.*, a complexation reaction between Hg$^{2+}$ and dithizone was measured on a distance-based paper device. However, dithizone could react with other heavy metals (Zn, Pb, Ni, Co) to form an insoluble colored product. Therefore, pH needed to be controlled in the method developed by Cai *et al.*

To increase the sensitivity of the fluorescent distance-based paper device, heating preconcentration was used (Fig. S9†).[35] The sample solution (2.0 mL) was loaded on the sample zone and heated to 100 °C for 1 hour. Then the concentrated analytes were injected into the fluorescent distance-based paper device using 75 μL of DI water as the elution solvent. After the heating preconcentration step, the naked eye detection limit (LOD) was found to be 5 μg L$^{-1}$ under UV lamp (Fig. 6), giving an enrichment factor of 100. Under the optimum conditions with heating preconcentration, the linear range of Hg$^{2+}$ concentration was in the range of 5 to 1000 μg L$^{-1}$ ($R^2 = 0.9951$, Fig. 6) compared to 0.5 to 25 mg L$^{-1}$ (500–25 000 μg L$^{-1}$) without preconcentration. The relative standard deviations (%RSD) at 50 and 500 μg L$^{-1}$ were 15.2% and 8.8%, respectively ($n = 7$), which is acceptable for paper-based devices.

A comparison between the analytical performance of this method and some previous paper-based sensors for the determination of Hg$^{2+}$ is shown in Table 2. Our proposed method gave a lower detection limit compared to other read-by-eye quantification methods. Furthermore, the signal obtained by our method is pH-independent so we can apply this method to

**Table 1** Determination of Hg$^{2+}$ in water samples ($n = 3$)$^a$

| Samples | Spiked level (mg L$^{-1}$) | Proposed method | | HG-AAS | |
|---|---|---|---|---|---|
| | | Hg(II) found (mg L$^{-1}$) | Recovery (%) | Hg(II) found (mg L$^{-1}$) | Recovery (%) |
| Drinking water | 0.00 | ND | | ND | |
| | 2.00 | 1.74 ± 0.50 | 87 | 1.74 ± 0.28 | 87 |
| | 12.00 | 11.67 ± 1.15 | 97 | | |
| | 22.00 | 20.26 ± 0.50 | 92 | | |
| Pond water | 0.00 | ND | | ND | |
| | 2.00 | 1.61 ± 0.76 | 80 | 1.86 ± 0.05 | 93 |
| | 12.00 | 13.29 ± 0.58 | 111 | | |
| | 22.00 | 19.99 ± 0.58 | 91 | | |
| Tap water | 0.00 | ND | | ND | |
| | 2.00 | 1.88 ± 0.29 | 94 | 1.82 ± 0.07 | 91 |
| | 12.00 | 12.35 ± 0.29 | 103 | | |
| | 22.00 | 20.13 ± 1.04 | 92 | | |

$^a$ ND = not detected.

**Table 2** Summary of $Hg^{2+}$ detection on paper-based analytical devices

| Method | Measurement | Linearity ($\mu g\ mL^{-1}$) | LOD ($\mu g\ mL^{-1}$) | Conditions | Lifetime | Sample | Ref. |
|---|---|---|---|---|---|---|---|
| AgNPls | Colorimetric, Photoshop | 5–75 | 0.12 | Added $CuSO_4$, boiling | — | Drinking and tap water | 52 |
| Pyridylazo indicators | Colorimetric, Photoshop | — | 10 | pH 6.5 | Over 2 months | Sewage water | 53 |
| SPR of ssDNA modified AuNPs | Colorimetric, ImageJ | 0–0.02 | 0.01 | pH 9 | Added NaCl (protected aggregation) | Pond and river water | 54 |
| Curcumin nanoparticles | Colorimetric, Photoshop | 0.01–0.4 | 0.003 (addition 50 times) | pH 7, phosphate buffer | Over 6 months in solution | Tap and waste water | 55 |
| AgNPs, double layer | Colorimetric, ImageJ | 0.05–7 | 1 | — | — | Drinking and tap water | 56 |
| PtNPs and TMB | Colorimetric, electrical readout system | 0.005–0.1 | 0.002 | — | Over 6 months in solution | Pond and tap water | 57 |
| Dithizone in NaOH | Distance-based | 1–30 | 0.93 | pH 9, added masking agent | Over 7 days | Whitening, cream | 32 |
| Silicon nanocrystals and carbon dots | Ratiometric fluorescent (semi-quantitative) | 0–0.02 (repeated 20 times reagent) | 0.002 | — | — | Tap and lake water | 58 |
| AgNPs | Colorimetric, smartphone application | 0–0.004 | 0.002 | — | — | River water | 59 |
| Nitrogen doped carbon dots (EDTA) | Fluorescence quenching, ImageJ | 0.02–10 | 0.02 | pH 4–9 | Added NaCl for stability | Tap water in solution (not apply in paper device) | 48 |
| Nitrogen-doped carbon dots (ethyle-nediamine) | Fluorescence quenching, distance-based | 0.005–1 | 0.005 | No effect (pH 3–11) | Over 5 months on paper | Drinking, pond and tap water | Our work |

samples in various pHs as an alternative for on-site quantification of trace $Hg^{2+}$ levels.

### 3.6. Application in water samples

The proposed method was successfully applied for the detection of $Hg^{2+}$ in drinking, pond, and tap water samples (Table 1). The recoveries of the spiked samples were in the range of 80–111% which is consistent with recommendations of the Association of Official Analytical Chemists (AOAC).[51] The method was also validated by HG-AAS. There was no significant difference between the two methods at 95% confidence interval which shows that the fluorescent distance-based paper device method is reliable and robust (Table S1†).

### 3.7. Stability of NCDs on distance-based device

For on-site monitoring, it is necessary for devices to remain stable over time. Hence, we studied the stability of devices after storing the prepared paper devices with NCDs for 5 months. The reagent solutions were coated on paper devices and allowed dry before storage at 4 °C in a Ziplock bag. After sample addition, the results were measured by naked eye under black light illumination. There was no significant difference between freshly prepared paper devices and stored

devices (ANOVA, $p > 0.05$ in Table S2†). As shown in Fig. S11b,† the distance signal decreased by 9%. Thus, the devices can be kept over 5 months (150 days). Moreover, the lifetime of NCDs on fluorescence distance-based devices is longer than in solution. The results of NCDs in solution showed that the distance signal was reduced by 20% of the original signal after one month which was caused by agglomeration of the NCD particles (Fig. S11a†).

## 4. Conclusion

A distance-based $Hg^{2+}$ quantification method using carbon nanodots and heating preconcentration on a paper-based device was developed for the first time. A $Bi^{3+}$ solution was used to improve the limit of detection. Under the optimum conditions with heating preconcentration, the naked eye detection limit (LOD) was 5 $\mu g\ L^{-1}$. Our device is the first strip test with naked-eye detection of trace levels of $Hg^{2+}$. The method has benefits of simplicity, inexpensive material and device fabrication, portability, robustness, high sensitivity and selectivity, and good performance in real water samples. This technology is a first step toward the detection of other trace heavy metals in food and the environment.

## Conflicts of interest

There are no conflicts to declare.

## Acknowledgements

## References

1 Metal: Chemical Properties and Toxicity, http://www.ilocis.org/documents/chpt63e.htm, accessed Dec 15, 2019.

2 M. Oves, M. S. Khan, A. H. Qari, M. N. Felemban and T. Almeelbi, *J. Biorem. Biodegrad.*, 2016, **7**, 1000334.

3 V. Mudgal, N. Madaan, A. Mudgal, R. B. Singh and S. Mishra, *Open Nutraceuticals J.*, 2014, **3**, 94–99.

4 F. Fernández-luqueño, F. López-valdez, P. Gamero-melo, S. Luna-, E. N. Aguilera-gonzález, A. I. Martínez, M. S. García-, G. Hernández-martínez, R. Herrera-mendoza and M. A. Álvarez-, *Afr. J. Environ. Sci. Technol.*, 2013, **7**, 567–584.

5 V. Masindi and K. L. Muedi, Environmental Contamination by Heavy Metals, *Heavy Met.*, Intechopen, 2018, pp. 155–133.

6 L. Järup, *Br. Med. Bull.*, 2003, **68**, 167–182.

7 M. Jaishankar, T. Tseten, N. Anbalagan, B. B. Mathew and K. N. Beeregowda, *Interdiscip. Toxicol.*, 2014, **7**, 60–72.

8 V. K. Gupta, I. Ali and H. Y. Aboul-Enein, *Dev. Environ. Sci.*, 2007, **5**, 33–56.

9 AOAC, *Heavy Metals in Food: Inductively Coupled Plasma–Mass Spectrometry*, AOAC Official Method, 2015, pp. 1–15.

10 WHO Mercury in Drinking-water, *Guidelines for Drinking-water Quality*, World Health Organization, Geneva, 1996, pp. 1–11.

11 U.S. Environmental Protection Agency, *Determination of Trace Elements in Water by Preconcentration and Inductively Coupled*, Plasma-Mass Spectrometry, Washington, 1997, pp. 1–59.

12 P. Ncube, R. W. M. Krause, D. T. Ndinteh and B. B. Mamba, *Water SA*, 2014, **40**, 175–182.

13 S. M. Ng, M. Koneswaran and R. Narayanaswamy, *RSC Adv.*, 2016, **6**, 21624–21661.

14 T. Itoh, *Chem. Rev.*, 2012, **112**, 4541–4568.

15 Y. Zhang, P. Cui, F. Zhang, X. Feng, Y. Wang, Y. Yang and X. Liu, *Talanta*, 2016, **152**, 288–300.

16 J. He, H. Zhang, J. Zou, Y. Liu, J. Zhuang, Y. Xiao and B. Lei, *Biosens. Bioelectron.*, 2016, **79**, 531–535.

17 S. Liu, J. Tian, L. Wang, Y. Zhang, X. Qin, Y. Luo, A. M. Asiri, A. O. Al-Youbi and X. Sun, *Adv. Mater.*, 2012, **24**, 2037–2041.

18 W. Lu, X. Qin, S. Liu, G. Chang, Y. Zhang, Y. Luo, A. M. Asiri, A. O. Al-Youbi and X. Sun, *Anal. Chem.*, 2012, **84**, 5351–5357.

19 J. Tian, Q. Liu, A. M. Asiri, A. O. Al-Youbi and X. Sun, *Anal. Chem.*, 2013, **85**, 5595–5599.

20 V. Georgakilas, J. A. Perman, J. Tucek and R. Zboril, *Chem. Rev.*, 2015, **115**, 4744–4822.

21 H. Li, Z. Kang, Y. Liu and S. T. Lee, *J. Mater. Chem.*, 2012, **22**, 24230–24253.

22 G. Sriram, M. P. Bhat, P. Patil, U. T. Uthappa, H. Y. Jung, T. Altalhi, T. Kumeria, T. M. Aminabhavi, R. K. Pai, Madhuprasad and M. D. Kurkuri, *TrAC, Trends Anal. Chem.*, 2017, **93**, 212–227.

23 Y. Lin, D. Gritsenko, S. Feng, Y. C. Teh, X. Lu and J. Xu, *Biosens. Bioelectron.*, 2016, **83**, 256–266.

24 W. Dungchai, O. Chailapakul and C. S. Henry, *Analyst*, 2011, **136**, 77–82.

25 N. Ratnarathorn, O. Chailapakul, C. S. Henry and W. Dungchai, *Talanta*, 2012, **99**, 552–557.

26 P. Rattanarat, W. Dungchai, D. Cate, J. Volckens, O. Chailapakul and C. S. Henry, *Anal. Chem.*, 2014, **86**, 3555–3562.

27 J. Noiphung, T. Songjaroen, W. Dungchai, C. S. Henry, O. Chailapakul and W. Laiwattanapaisal, *Anal. Chim. Acta*, 2013, **788**, 39–45.

28 W. Dungchai, O. Chailapakul and C. S. Henry, *Anal. Chem.*, 2009, **81**, 5821–5826.

29 T. Songjaroen, W. Dungchai, O. Chailapakul, C. S. Henry and W. Laiwattanapaisal, *Lab Chip*, 2012, **12**, 3392–3398.

30 K. Yamada, D. Citterio and C. S. Henry, *Lab Chip*, 2018, **18**, 1485–1493.

31 Y. Kim, G. Jang and T. S. Lee, *ACS Appl. Mater. Interfaces*, 2015, **7**, 15649–15657.

32 L. Cai, Y. Fang, Y. Mo, Y. Huang, C. Xu, Z. Zhang and M. Wang, *AIP Adv.*, 2017, **7**, 085214–085218.

33 Water quality association, https://www.wqa.org/learn-about-water/common-contaminants/aluminum, accessed Jul 15, 2019.

34 C. W. Quinn, D. M. Cate, D. D. Miller-Lionberg, T. Reilly, J. Volckens and C. S. Henry, *Environ. Sci. Technol.*, 2018, **52**, 3567–3573.

35 S. Y. Wong, M. Cabodi, J. Rolland and C. M. Klapperich, *Anal. Chem.*, 2014, **86**, 11981–11985.

36 A. Beiraghi and S. A. Najibi-Gehraz, *Sens. Actuators, B*, 2017, **253**, 342–351.

37 K. Phoonsawat, N. Ratnarathorn, C. S. Henry and W. Dungchai, *Analyst*, 2018, **143**, 3867–3873.

38 APHA, *Standard Methods for the Examination of Water and Wastewater*, American Public Health Association, 1992, pp. 3–33.

39 X. Sun and Y. Lei, *TrAC, Trends Anal. Chem.*, 2017, **89**, 163–180.

40 S. S. J. Xavier, G. Siva, J. Annaraj, A. R. Kim, D. J. Yoo and G. G. Kumar, *Sens. Actuators, B*, 2018, **259**, 1133–1143.

41 R. Tabaraki and N. Sadeghinejad, *Ecotoxicol. Environ. Saf.*, 2018, **153**, 101–106.

42 Y. Zhang, N. Jing, J. Zhang and Y. Wang, *Int. J. Environ. Anal. Chem.*, 2017, **97**, 841–853.

43 S. Chandra, A. R. Chowdhuri, T. K. Mahto, D. Laha and S. K. Sahu, *Nano-Structures & Nano-Objects*, 2017, **12**, 10–18.

44 R. Liu, H. Li, W. Kong, J. Liu, Y. Liu, C. Tong, X. Zhang and Z. Kang, *Mater. Res. Bull.*, 2013, **48**, 2529–2534.

45 Y. Guo, L. Zhang, S. Zhang, Y. Yang, X. Chen and M. Zhang, *Biosens. Bioelectron.*, 2015, **63**, 61–71.

46 J. Hua, J. Yang, Y. Zhu, C. Zhao and Y. Yang, *Spectrochim. Acta, Part A*, 2017, **187**, 149–155.

47 D. Yoo, Y. Park, B. Cheon and M. H. Park, *Nanoscale Res. Lett.*, 2019, **14**, 272.

48 K. Patir and S. K. Gogoi, *Nanoscale Adv.*, 2019, **1**, 592–601.

49 N. Jeromiyas, E. Elaiyappillai, A. S. Kumar, S. T. Huang and V. Mani, *J. Taiwan Inst. Chem. Eng.*, 2019, **95**, 466–474.

50 S. Chaiyo, A. Apiluk, W. Siangproh and O. Chailapakul, *Sens. Actuators, B*, 2016, **233**, 540–549.

51 AOAC, *Guidelines for Single Laboratory Validation of Chemical Methods for Dietary Supplements and Botanicals*, AOAC Official, 2002, pp. 1–38.

52 A. Apilux, W. Siangproh, N. Praphairaksit and O. Chailapakul, *Talanta*, 2012, **97**, 388–394.

53 L. Feng, X. Li, H. Li, W. Yang, L. Chen and Y. Guan, *Anal. Chim. Acta*, 2013, **780**, 74–80.

54 G. Chen, W. Chen, Y. Yen, C. Wang, H. Chang and C. Chen, *Anal. Chem.*, 2014, **86**, 6843–6849.

55 S. R. N. Pourreza and H. Golmohammadi, *RSC Adv.*, 2016, **6**, 69060–69066.

56 R. Meelapsom, P. Jarujamrus, M. Amatatongchai, S. Chairam, C. Kulsing and W. Shen, *Talanta*, 2016, **155**, 193–201.

57 W. Chen, X. Fang, H. Li, H. Cao and J. Kong, *Sci. Rep.*, 2016, **6**, 1–7.

58 X. Guo, C. Liu, N. Li and S. Zhang, *R. Soc. Open Sci.*, 2018, **5**, 171922.

59 M. L. Firdaus, A. Aprian, N. Meileza, M. Hitsmi, R. Elvia, L. Rahmidar and R. Khaydarov, *Chemosensors*, 2019, **7**, 1–9.